Novel function of nucleus accumbens in motor control during recovery after spinal cord injury

Masahiro Sawada[1,2], Kenji Kato[1,3], Takeharu Kunieda[2], Nobuhiro Mikuni[4], Susumu Miyamoto[2], Hirotaka Onoe[5], Tadashi Isa[1,3], Yukio Nishimura[1,3,6]*

[1]Department of Developmental Physiology, National Institute for Physiological Sciences, Okazaki 444-8585, Japan.

[2]Department of Neurosurgery, Graduate School of Medicine, Kyoto University, Kyoto 606-8507, Japan.

[3]Department of Physiological Sciences, School of Life Science, The Graduate University for Advanced Studies, SOKENDAI, Hayama 240-0193, Japan.

[4]Department of Neurosurgery, Sapporo Medical University, Sapporo 060-8543, Japan.

[5]Division of Bio-Function Dynamics Imaging, RIKEN Center for Life Science Technologies, Kobe 650-0047, Japan.

[6]Precursory Research for Embryonic Science and Technology, Japan Science and Technology Agency, Tokyo 102-0076, Japan.

* To whom correspondence should be addressed. E-mail: yukio@nips.ac.jp

Motivation facilitates recovery after neuronal damage, but its mechanism is elusive. It is generally thought that the nucleus accumbens (NAc) regulates motivation-driven effort, but is not involved in the direct control of movement. Using causality analysis we identified the flow of activity from NAc to the sensorimotor cortex (SMC) during recovery of dexterous finger movements after spinal cord injury at cervical level in macaque monkeys. Furthermore, reversible pharmacological inactivation of NAc during the early recovery period diminished high-frequency oscillatory activity in the SMC, which was accompanied by a transient deficit of amelioration in finger dexterity obtained by rehabilitation. These results demonstrate that during recovery after spinal damage, the NAc up-regulates the high frequency activity of the SMC and is directly involved in the control of finger movements.

One Sentence Summary: nucleus accumbens, which is a motivation center, up-regulates the activity of the sensorimotor cortex for the recovery from spinal cord injury.

Motivation enhances and depression impedes functional recovery after neuronal damages (*1-2*). However, the mechanism underlying this psychological effect on recovery remains obscure. The nucleus accumbens (NAc) plays a critical role in processing motivation to obtain reward (*3-6*). A large fraction of neurons in the NAc reflects the availability of reward and vigor of subsequent approach to a target (*7*). However, NAc is not thought to be directly involved in the control of motor functions such as finger dexterity. It has been reported that NAc controls locomotion (*8, 9*), however, it might be through regulation of vigor (*10-12*). On the other hand, in functional brain imaging studies in nonhuman primates, the activity of the NAc during reach and grasp task was increased in association with the primary motor cortex (M1) during recovery from the partial spinal cord injury (SCI), which had not been observed before the injury (*13, 14*). These studies suggest that the interaction between NAc and M1 plays a pivotal role in the recovery of finger dexterity. However, the causal relationship between the neural activities of M1, NAc and functional recovery remains obscure. In this study, we investigated the interaction between the neuronal activities of NAc and M1.

After sufficient reach and grasp task training (Fig. 1A), four macaque monkeys were subjected to SCI, which was limited to the C4/5 level of the lateral corticospinal tract (Fig. 1B and fig. S3). Finger dexterity was immediately impaired in the three monkeys who had relatively large lesions (Monkeys M, T, and R; Fig. 1B and fig. S3). Consistent with recent lesion studies (*15-17*), recovery of the precision grip exceeded 90% within 100 days in monkeys whose finger dexterity was impaired immediately after SCI. ‘Early stage’ recovery was defined as the period from SCI to the time point on which the success rate reached 100% for two successive days. ‘Late stage’ recovery was defined as the period after which the grip success rate remained repeatedly at 100%

(Fig. 1B, 3B and Movie S1). Finger dexterity was not markedly impaired in Monkey D, presumably because the SCI was comparatively small (fig. S3).

To evaluate the potential of the NAc to motivate recovery we determined the relationship between NAc and M1 activity during the two stages of behavioral recovery and compared with the pre-SCI stage. We examined oscillatory activity of the two regions while the monkey performed a reach and grasp task requiring dexterous finger movements at various time points before and after SCI in two monkeys (Monkeys T and R, in which we conducted simultaneous recordings of ECoG on the sensorimotor cortex (SMC) and LFPs in the NAc (Fig. 1C). During the early stage and late stage recovery, time-frequency analysis of M1 activity showed long lasting high-frequency gamma activity (115–400 Hz) through the period of reach and grasp movements, compared with that observed before SCI (Fig. 1D, upper row and E). The high-frequency component of NAc at early stage appeared to have reached the similar level as the pre-SCI (Fig. 1D, lower row and F). On the other hand, low frequency component in the NAc during the early recovery stage showed significant decrease during reaching and grasping (Fig. 1E). We successively employed Granger causality analysis (GCA) (*18-20*) to evaluate the directionality of interactions between M1 and NAc activity in the two monkeys. GCA demonstrated an increased signal flow from the NAc to M1 in the high-gamma band (115–400 Hz) during early stage recovery (Fig. 2A, middle-upper). In the late stage recovery, the signal flow from the NAc to M1 was diminished (Fig. 2A, right-upper). Compared with observations before SCI, or during late stage recovery, the signal flow from the NAc to the global SMC was much stronger (Fig. 2C).

Despite these analyses it remained unclear whether NAc is a critical modulator of SMC activity. We therefore injected muscimol at various time points before and after SCI to induce a temporary unilateral blockade of the NAc in the contralesional hemisphere. We tested the effects

of NAc inactivation on finger dexterity in all the four monkeys, and on SMC brain activity in three monkeys (Monkeys M, T, and R; see Methods in supplementary materials). In the three monkeys with SCI-induced impaired finger dexterity, NAc inactivation exacerbated the grasping deficits during the early recovery stage (Fig. 3A to C and Movie S2). The same manipulation caused no remarkable deficit during either the pre-SCI period (Fig. 3A to C and Movie S3) or the late recovery stage (Fig. 3B, C and Movie S4). Importantly, despite their additional early-stage motor impairment the monkeys' intention to obtain food was undiminished. During the inactivation, monkeys would try to pick up a piece of food they had dropped, and could retrieve it using the contralesional hand (fig. S6A and Movie S5). Accompanying the impaired precision grip success rate of monkeys M, T and R, their movement time for grasping was also prolonged only during the early stage in all these animals (Fig. 3D). NAc inactivation tended to prolong the reaching time, but due to the limited number of animals and intrinsic variability, no statistical significance was reached (Fig. 3E). After SCI, reaching was relatively unaffected following NAc inactivation, presumably because the pathways involved in the control of reaching (via cortico-propriospinal (*17, 21*) and cortico-reticulospinal tracts (*22*)) mostly remained intact. Furthermore, inactivation of the ipsilesional NAc caused no additional effect on the lesion-affected finger dexterity (fig. S6B). Similarly, NAc inactivation had no obvious effect on finger dexterity before or after SCI in the monkey D who had no clear impairment in finger dexterity after SCI (fig. S3).

In the three monkeys with lesion-impaired grasping (M, T and R) we explored changes in M1 activity induced by NAc inactivation (Fig. 4A). Before the SCI no change in cortical activity was observed following NAc inactivation (Pre-SCI on the left column of Fig. 4B, Pre-SCI of Fig. 4D, Pre-SCI on the left column of fig. S4A and B). However, during the early stage of recovery, NAc inactivation attenuated high-frequency gamma activity (115–400 Hz), while lower-frequency

gamma (50–100 Hz) tended to be enhanced (Early on the middle column of Fig. 4B, Early of Fig.4D, Early on the middle column of fig. S4A and B). This result was consistent with that gamma band in NAc decreased during early stage. During late stage recovery, NAc inactivation had no clear effect on the SMC-ECoG signals (Late on the right column of Fig.4B, Late of Fig. 4D, Late on the right column of fig. S4A and B). These results accompanied the finding that finger dexterity was also unaffected by NAc inactivation during the late stage of recovery.

It is widely accepted that high-gamma band activity reflects synchronized firing of a neural population near the electrode (*23, 24*). Our finding that the disappearance of high-gamma activity (115–400Hz) occurred in association with disturbed finger dexterity suggests that high-frequency oscillatory activity of M1, which was interrupted by NAc inactivation, played a critical role in the control of dexterous finger movements during recovery. Additionally, we observed that this oscillatory modulation occurred across all areas of the SMC, including the premotor cortex (PM), M1, and primary somatosensory cortex (S1). Before NAc inactivation, both high-frequency gamma (115–400Hz) and lower-frequency gamma (50–100Hz) bands were observed in the dorsolateral SMC (Fig. 4C, fig. S5A and B). However, following NAc inactivation, the reduction in high-frequency gamma power and the increase in lower-frequency gamma power occurred on all of the electrodes in SMC (Fig. 4B, fig. S5A and B).

In this study, we have demonstrated that NAc inactivation produced severe deficits in finger movement during the early stage recovery. This suggests that the NAc makes a direct contribution to motor performance during the early stage recovery after SCI. This conclusion is supported by the finding that NAc inactivation significantly suppressed high-frequency oscillatory activity in the SMC. Other investigations have shown that the NAc plays a pivotal role in maintaining the motivation to obtain reward when required to expend more effort (*4-6*). Indeed,

rats with NAc lesions switched to choosing low-value reward at low costs, rather than choose high-value/high-cost reward (*4*). In our study, possibly several planning and/or executing centers - including the motor cortex - require a higher level of activity for the execution of the same movement after SCI. This idea might be similar to what has been described by Brodal as "mental energy" in his self-observation after stroke (*25*). Therefore, during the early-stage of recovery, the monkeys would have to exert more motivational effort to achieve the precision grip. When the recovery was almost complete, such extra effort would no longer be necessary. The pathways from the NAc to the SMC remain unclear. However it has been shown that the NAc provides multi-synaptic (minimally disynaptic) projection to all the body-part representations in the M1 presumably through the basal forebrain cholinergic neurons (*26-28*). On the other hand, there exists a pathway from the ventral tegmental area, which receives dense inputs from the NAc, to the SMC (*29*).

Because the motor recovery after the same SCI was shown to be training-dependent (*30*), it would be reasonable to suggest that the NAc contributes to recovery after SCI from the present results. Our findings suggest that NAc could be a critical target for therapeutic interventions that aim to enhance the motivation of patients with SCIs, and thereby promote their recovery. This idea may apply to a broad range of neurological disorders, including stroke, traumatic brain injuries etc.

142 References and Notes:

143 1. E. Chemerinski, R. G. Robinson, J. T. Kosier, *Stroke* **32**, 113–117 (2001).

144 2. S. K. Saxena, T. P. Ng, G. Koh, D. Yong, N. P. Fong, *Acta Neurol.Scand*. **115**, 339–346 (2007).

145 3. E. S. Chantal, E. P. Richard, *Behav. Brain Res*. **61**, 9 – 21 (1994).

146 4. R. N. Cardinal, D. R. Pennicott, C. L. Sugathapala, T. W. Robbins, B. J. Everitt, *Science* **292**,
147 2499-2501 (2001).

148 5. R. N. Cardinal, J. A. Parkinson, J. Hall, B. J. Everitt, *Neurosci. Biobehav. Rev.* **26**, 321–352
149 (2002).

150 6. J. D. Salamone, M. Correa, A. Farrar, S. M. Mingote, *Psychopharmacology (Berl.)* **191**, 461–
151 482 (2007).

152 7. V. B. McGinty, S. Lardeux, S. A. Taha, J. J. Kim, S. M. Nicola, *Neuron* **78**, 910–922 (2013).

153 8. L. E. Annett, R. M. Ridley, S. J. Gamble, H. F. Baker, *Psychopharmacology (Berl.)* **99**, 222–
154 229 (1989)

155 9. S. Ikemoto, B. M. Witkin, *Synapse* **47**, 117–122 (2003)

156 10. M. Amalric, G. F. Koob, *Neurosci.* **7**, 2129–2134 (1987).

157 11. V. J. Brown, E. M. Bowman, *Eur. J. Neurosci*. **7**, 2479–2485 (1995).

158 12. C. Giertler, I. Bohn, W. Hauber, *Behav. Pharmacol*. **15**, 55–63 (2004).

159 13. Y. Nishimura et al., *Science* **318**, 1150–1155 (2007).

160 14. Y. Nishimura et al., *PLoS One* **6**, e24854 (2011).

161 15. S. Sasaki, et al., *J. Neurophysiol.* **92**, 3142–3147 (2004).

16. Y. Nishimura, Y. Morichika, T. Isa, *Brain* **132**, 709–721 (2009).

17. B. Alstermark, T. Isa, *Annu. Rev. Neurosci*. **35**, 559–578 (2012).

18. A. Brovelli et al., *Proc. Natl. Acad. Sci. USA* **26**, 9849–9854 (2004).

19. C. Bernasconi et al., *Biol. Cybern*. **3**, 199–210 (1999).

20. W. Hesse et al., *J. Neurosci. Methods* **124**, 27–44 (2003).

21. M. Kinoshita et al., *Nature* **487**, 235-238 (2012).

22. D. G. Lawrence, H. G. Kuypers, *Brain* **91**, 1–14 (1968).

23. R. Supratim et al., *J. Neurosci.* **45**, 11526–11536 (2008).

24. E. C. Leuthardt, G. Schalk, J. R. Wolpaw, J. G. Ojemann, D. W. Moran, *J. Neural Eng*. **1**, 63–71 (2004).

25. A. Brodal, *Brain* **96**, 675–694 (1973).

26. S. Miyachi et al., *J. Neurosci.* **10,** 2547–2556 (2005).

27. S.Miyachi et al., *Neurosci. Res.* **56**, 300–308 (2006).

28. S. N. Haber et al., *Neuropsychopharmacology* **1**, 4–26 (2010).

29. A. Jonas et al., *J. Neurosci.* **7**, 2481–2487 (2011)

30. Y. Sugiyama et al., *J. Neurophysiol.* **109**, 2853-2865 (2013)

31. Z. C. Chao, Y. Nagasaka, N. Fujii, Front. Neuroeng. **30**, 3:3 (2010).

32. T. Yanagisawa et al., J. Neurosurg. **6**, 1715–1722 (2011).

33. Y. Murata et al., J. Neurosci. **35**, 84-95 (2015).

34. A. M. Partsalis, Y. Zhang, S. M. Highstein, J. Neurophysiol. **73**, 632-650 (1995).

35. R. Arikan et al., J. Neurosci. Methods **118**, 51-57 (2002).

36. J. M. Edeline et al., Neurobiol. Learn Mem. **1**, 100–124 (2002).

37. A. K. Seth, J. Neurosci. Methods **186**, 262–273 (2010).

38. Y. Sugiyama et al., J. Neurophysiol. **109** 2853-2865 (2013).

Acknowledgments: We thank P. Redgrave for comments on the manuscript, and Y. Itani, N. Takahashi, M. Togawa, and K. Isa for technical help. The monkeys used in this study were provided by the National Institute of Natural Sciences through the National Bio-resource Project of MEXT, Japan. This work was supported by grants from the “Brain Machine Interface Development” and performed under the Strategic Research Program for Brain Sciences and Precursory Research for Embryonic Science and Technology, Japan Science and Technology Agency to Y.N., a Grant-in-Aid for Scientific Research on Innovative Areas "Adaptive circuit shift" to T.I. (Project No. 26112008) and H.O. (26112003) and the Grant-in-Aid for Scientific Research from the Ministry of Education, Culture, Sports, Science and Technology of Japan to H.O. (KAKENHI (B) No. 24300196 and (A) No.15H01819). All data are stored at department of developmental physiology in National Institutes of Natural Sciences, Okazaki, Japan.

198 **Fig. 1.** Time course of recovery of finger dexterity and brain activity. (**A**) Reach and grasp. (**B**)
199 The time course of precision grip success rate in Monkey R. Black arrowheads indicate the days
200 corresponding to the recordings shown in **D**. The black shaded area in the inset indicates the site
201 of the spinal cord lesion. The percentage value beside the spinal cord illustration shows the
202 proportion of the tissue that has been lesioned. (**C**) Schematic drawing of simultaneous recording
203 of SMC-ECoG and NAc-LFP. (**D**) Time-frequencygram of M1 (upper panels) and NAc (lower
204 panels) activities in monkey R. Time 0; grasp onset. Green arrowheads; reach onset. Red
205 arrowheads; grasp end. Each panel is the average of 30 trials. (**E**) Population data of mean power
206 change compared with baseline period (-1.5 to -1.0 sec from grasp onset) in M1 during the
207 monkeys were grasping (0 to 0.5 sec from grasp onset. n; the number of simultaneous recording
208 session consisted of 30 trials across two monkeys (T and R) at each stage. Shading indicates the
209 S.E.M. Blue points on the graph: $P < 0.05$, one way ANOVA. See method. (**F**) Same as **E** but in
210 NAc.

Fig. 2. Directionality of activity interactions. (**A**) Representative time-frequencygram of GC during the task in Monkey R. Time alignment is the same as in Fig. 1**D**. Causal information flow from the NAc to M1 of each stage (upper panels) and from M1 to the NAc (lower panels). (**B**) GC population data from the NAc to M1 (upper panel) and from M1 to the NAc (lower panel) during the task, obtained across all recordings in two monkeys (T and R). The number means the total number of experimental days across the two monkeys. Shading indicates the standard error of the mean (S.E.M.). (**C**) GC networks. X and Y axis are source and sink of information, respectively.

Fig. 3. Temporal inactivation of the NAc caused additional impairment of dexterous finger control. (**A**) Retrieval of a piece of food before (Control) and during muscimol inactivation of the NAc (NAc inactivation) in Monkey M prior to (Pre-SCI) and 29 days after SCI (Early), respectively. Time (s) elapsed after the first panel is indicated below subsequent panels. (**B**) Success rate of precision grip prior to NAc inactivation (open circles) and following NAc inactivation (Red circles) in Monkey M. The light blue circles indicate results following a control injection of saline into the NAc (Saline). (**C**) Population data collected across all monkeys reveals the impairment of finger dexterity after SCI (Monkey M, T, and R) (paired t-test). (**D**) Increase in the mean grasping time caused by muscimol inactivation, or after saline injections into NAc at each experimental stage across monkey M, T, and R. Error bars indicate the S.E.M. See methods for statistical analysis. (**E**) Increase in mean reaching time. There was a trend of increase during the early stage, but due to the limited number of animals and intrinsic

Fig. 4. NAc inactivation disrupted cortical activity during the early stage recovery. (**A**) Schematic drawing of recording of SMC-ECoG during NAc inactivation. (**B**) Time-frequencygram of brain activity of the contralesional M1 while Monkey M performed the grasp task prior to (upper row) and during NAc inactivation (middle row). Time alignment in the map is the same as in Fig. 1**D**. Lower row indicates power change in M1 activity caused by NAc inactivation. Blue and red areas indicate statistically inactivated and activated components, respectively. (**C**) Topographical mapping of the intensity of gamma and high-gamma activity power before and during inactivation in Monkey M during the early stage (left and middle columns). Each dot on the maps indicates each electrocorticographic (ECoG) electrode. Right column indicates the mapping of power changes in gamma and high-gamma activity. CS: central sulcus. (**D**) Population data showing NAc inactivation-induced mean changes in power and S.E.M (shading) for each frequency across all electrodes in three monkeys. The number means the total number of experimental days across the three monkeys. Red points on the graph: $P < 0.05$, Post-hoc test between Early and Pre-SCI. See method.

245 Figure1

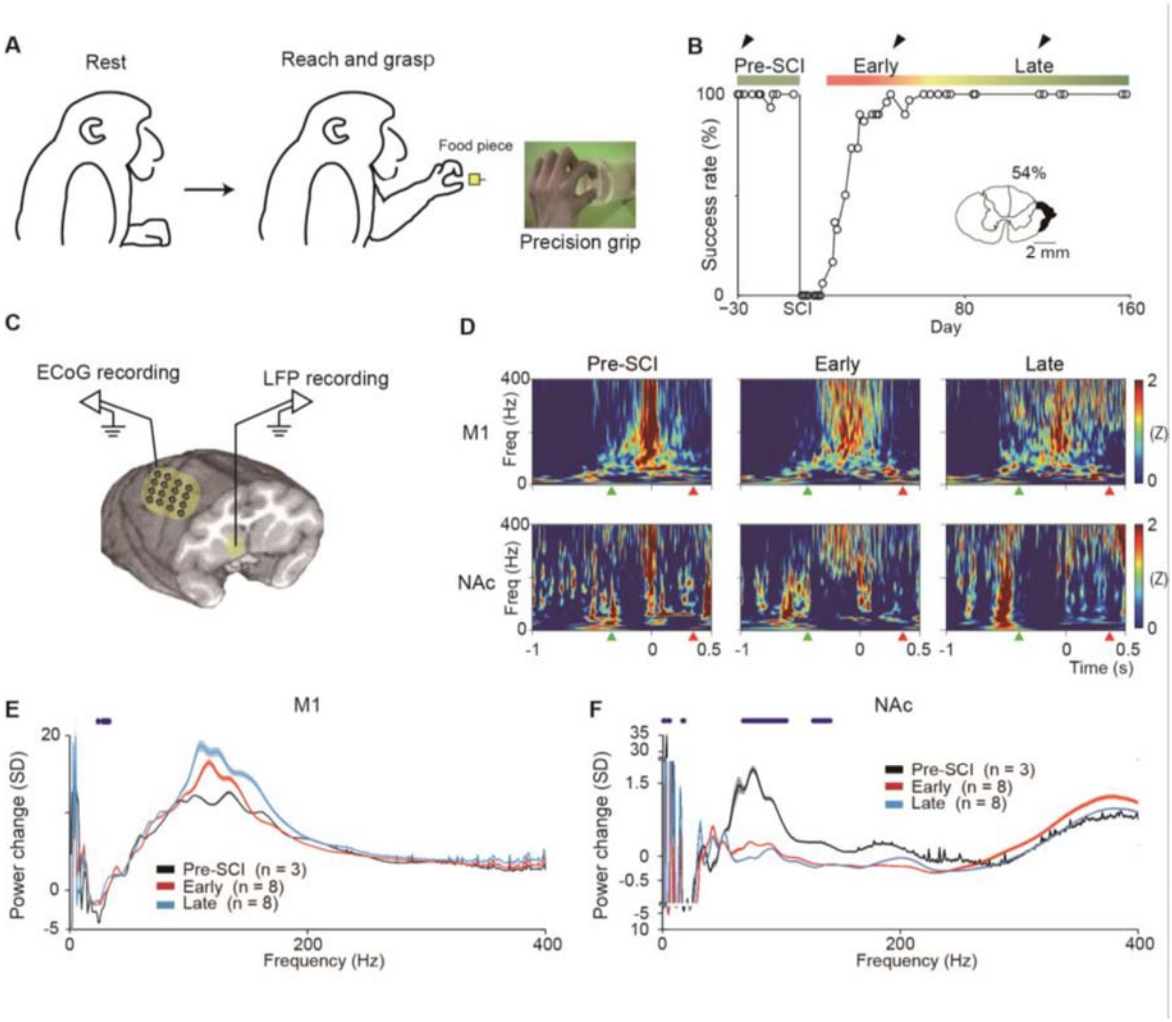

246

247

Figure 2

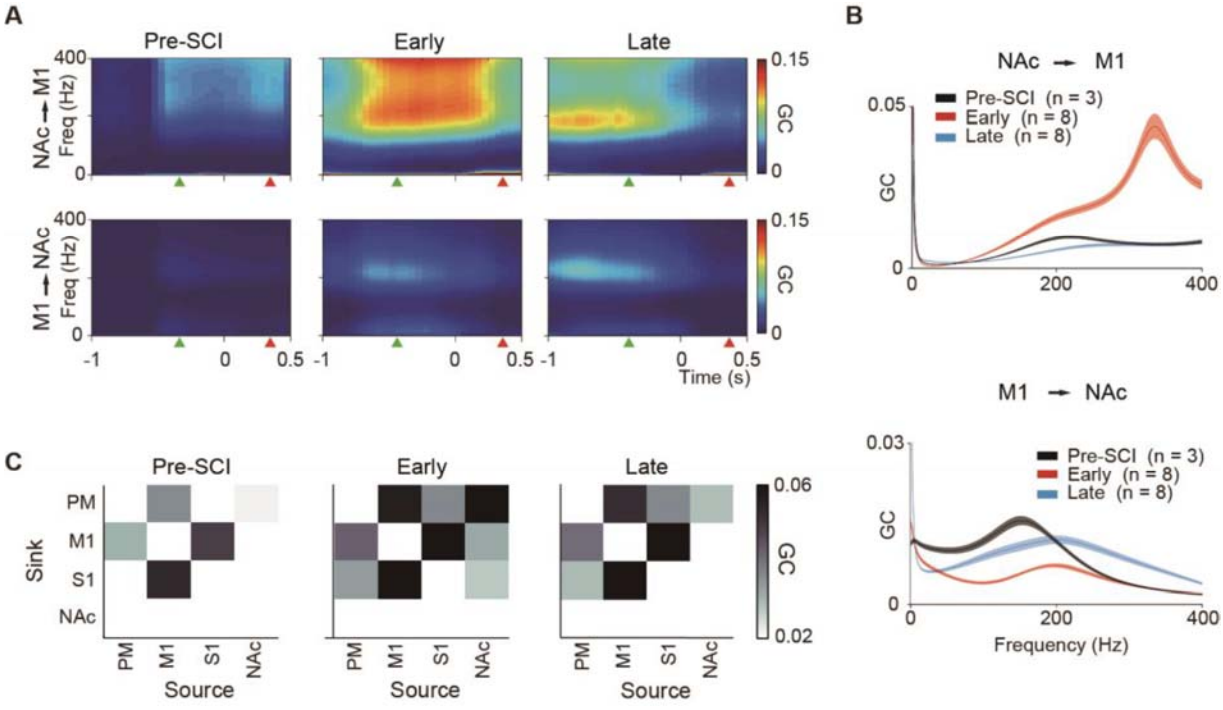
A
Pre-SCI
Early
Late
NAc → M1
Freq (Hz)
400
0
0.15
GC
0
M1 → NAc
Freq (Hz)
400
0
0.15
GC
0
-1
0
0.5
Time (s)
B
NAc → M1
Pre-SCI (n = 3)
Early (n = 8)
Late (n = 8)
0.05
GC
0
200
400
M1 → NAc
0.03
GC
0
200
400
Frequency (Hz)
C
Pre-SCI
Early
Late
Sink
PM
M1
S1
NAc
Source
0.06
GC
0.02

Figure 3

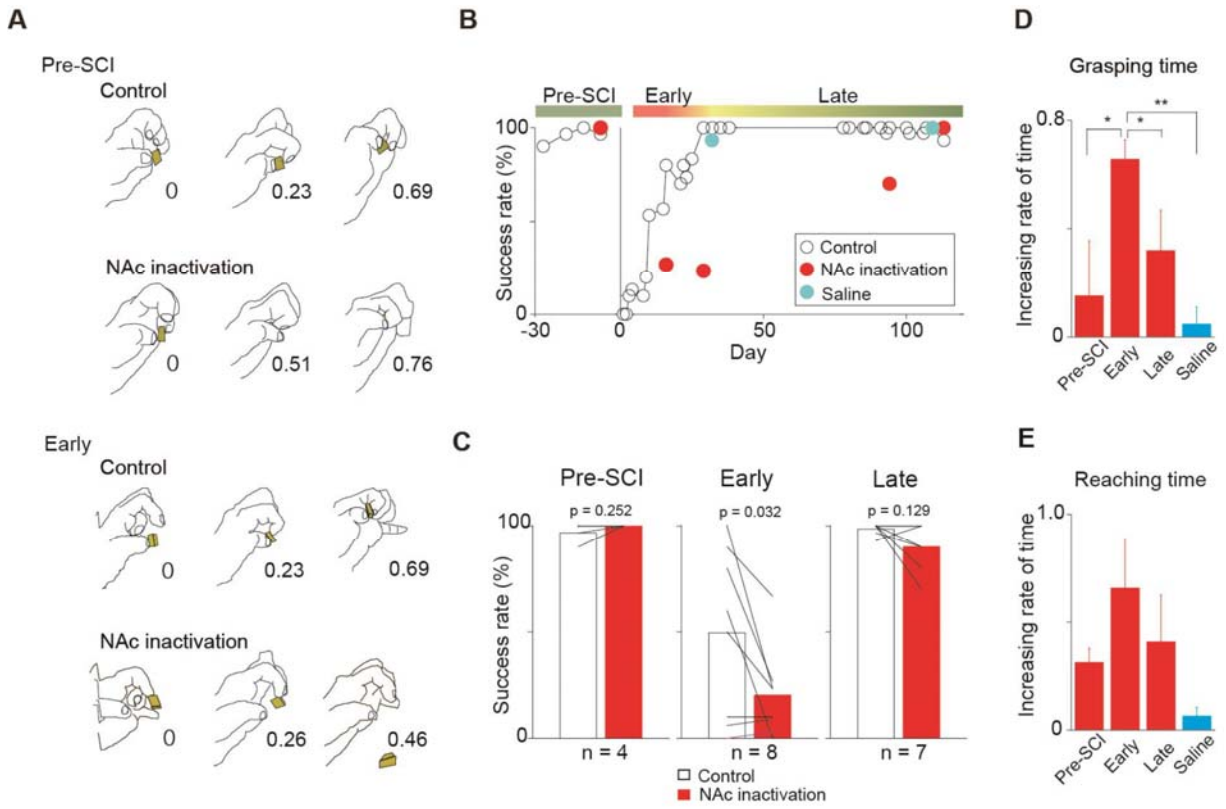
A
Pre-SCI
Control
0
0.23
0.69
NAc inactivation
0
0.51
0.76
Early
Control
0
0.23
0.69
NAc inactivation
0
0.26
0.46
B
Pre-SCI
Early
Late
100
Success rate (%)
0
-30
0
50
100
Day
Control
NAc inactivation
Saline
C
Pre-SCI
Early
Late
p = 0.252
p = 0.032
p = 0.129
100
Success rate (%)
0
n = 4
n = 8
n = 7
Control
NAc inactivation
D
Grasping time
0.8
Increasing rate of time
0
*
*
**
Pre-SCI
Early
Late
Saline
E
Reaching time
1.0
Increasing rate of time
0
Pre-SCI
Early
Late
Saline

Figure 4

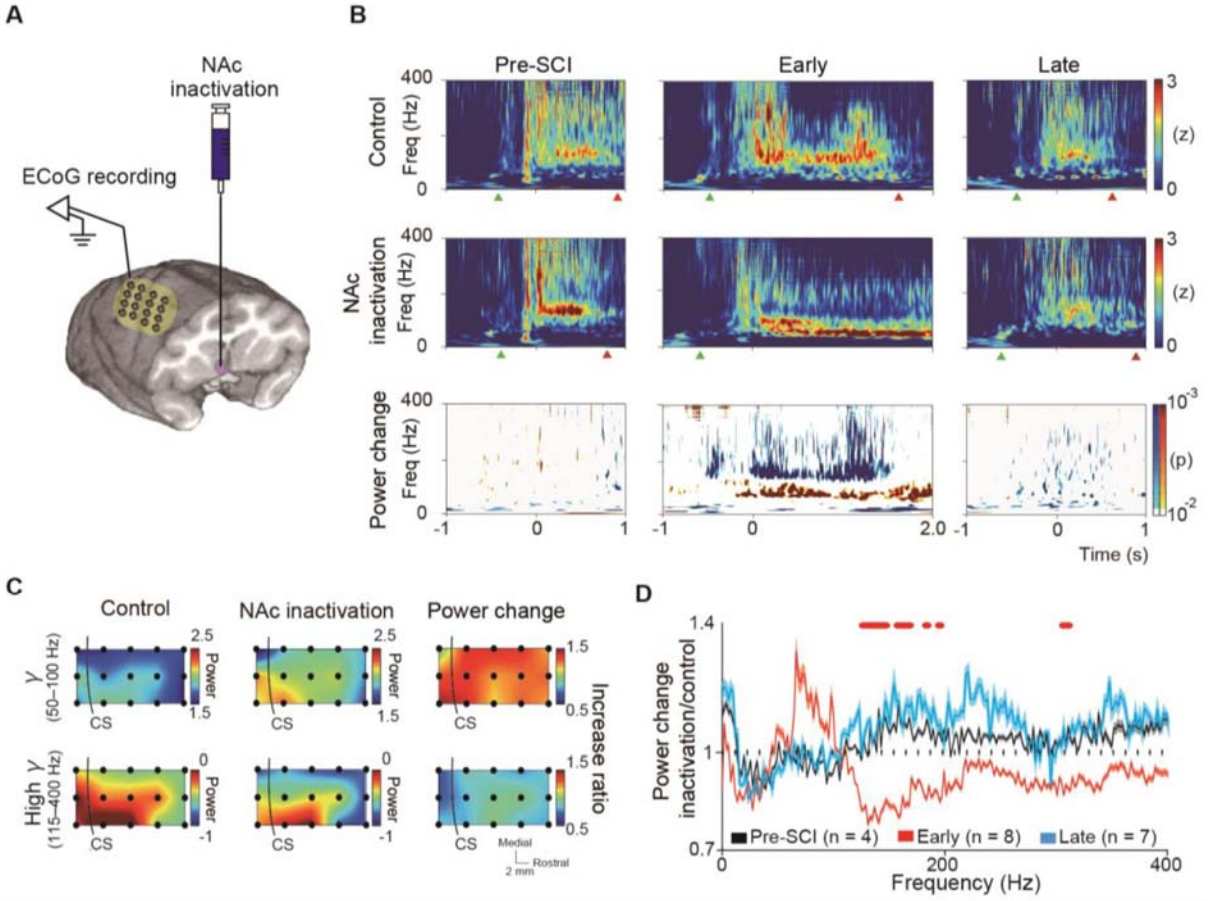
A
NAc inactivation
ECoG recording
B
Pre-SCI
Early
Late
Control
NAc inactivation
Power change
Freq (Hz)
400
0
3
(z)
10-3
(p)
10-2
-1
0
1
2.0
Time (s)
C
Control
NAc inactivation
Power change
γ (50–100 Hz)
High γ (115–400 Hz)
Power
2.5
1.5
0
-1
CS
Increase ratio
1.5
0.5
Medial
Rostral
2 mm
D
Power change inactivation/control
1.4
1
0.7
Pre-SCI (n = 4)
Early (n = 8)
Late (n = 7)
0
200
400
Frequency (Hz)

Supplementary Materials:

Materials and Methods

Figures S1-S6

Movies S1-S5

Supplementary Materials for

Novel function of nucleus accumbens in motor control during recovery after spinal cord injury

Masahiro Sawada, Kenji Kato, Takeharu Kunieda, Nobuhiro Mikuni, Susumu Miyamoto, Hirotaka Onoe, Tadashi Isa, Yukio Nishimura

Correspondence to: yukio@nips.ac.jp

This PDF file includes:

Materials and Methods
Figs. S1 to S6
Captions for Movies S1 to S5

Other Supplementary Materials for this manuscript includes the following:

Movies S1 to S5

Subjects

Four macaque monkeys (one Macaca mulatta and three Macaca fuscata, bodyweight 5.2–7.1 kg) were used in the present study. The experimental protocols followed the guidelines set forth by the Ministry of Education, Culture, Sports, Science and Technology (MEXT) of Japan, and were approved by the Institutional Animal Care and Use Committee of the National Institutes of Natural Sciences (Approval No. 14A126). All the four animals (Monkeys D, M, T, and R) were subjected to the NAc inactivation experiment. Monkeys M, T and R were used for ECoG recording from the SMC. Simultaneous recordings of ECoG from SMC and LFP from NAc were conducted in Monkeys T and R.

Behavioral task

To assess the finger dexterity, monkeys were trained to perform a reaching and grasping task. One monkey (Monkey D) was trained to sit in its home cage and reach for a cube of sweet potato ($5 \times 5 \times 5$ mm^3) through a window on the transparent acrylic front panel of the cage. The food was presented between an 8-mm-wide vertical slit, which was positioned at the height of the monkey's shoulder, and the monkey retrieved the morsel of sweet potatoes through the window. The other three monkeys (Monkeys M, T, and R) were trained to sit in a monkey chair with their heads fixed in a stereotaxic frame attached to the chair in front of a non-transparent gate on the acrylic front panel. Monkeys were required to put their left hand on a board positioned at the height of their abdomen. The gate was opened after the monkeys held their left hand on the board for at least 2 s. After the gate opened, the monkeys could retrieve a piece of food that was presented in the slit. Each recording session consisted of 30 trials. A digital video camera (33 frames/s) was used to record the reach-retrieval sequences from a lateral view. A successful trial was defined as any trial that resulted in a successful precision grip with the pads of the index finger and thumb, in addition to removal of the food from the pin without dropping it. The success rate was calculated as the number of successful trials divided by 30. We recorded the time from the onset of the hand movement to reaching the gate (Reaching time) and the time required to pick up the piece of food from the slit (Grasping time).

Surgeries

All surgeries described below were performed using sterilization under general anaesthesia, starting with a combination of ketamine (10 mg/kg, intramuscular injection [i.m.]) and xylazine (1 mg/kg, i.m.) and succeeded by intubation and isoflurane (1–1.5%) inhalation to maintain stable, deep anaesthesia throughout the surgery. Heart rate, peripheral capillary oxygen saturation and end-expiratory carbon dioxide pressure were monitored during the surgery. Ringer's solution was continuously administered through an intravenous (i.v.) drip. Dexamethasone (0.825 mg/ kg body weight) and ampicillin (40 mg/kg) were administered after anaesthesia.

1) Implantation of the electrocorticographic (ECoG) electrode array and chamber

We recorded oscillatory brain activities from the sensorimotor cortex (SMC), including the ventral and dorsal aspects of the premotor cortex, primary motor cortex, and somatosensory cortex. To do so, we used an ECoG electrode array. ECoG electrode arrays have advantages, as they are able to record cortical surface signals less invasively across broader regions compared with

331 microelectrode-based methods. Furthermore, the ECoG electrode array provided durable and
332 stable recordings, which was an important feature, as we conducted long-term recordings for more
333 than 4 months after SCI (*31-32*). In all monkeys, surgery was performed to gain easy access for
334 muscimol injections into the nucleus accumbens (NAc). A custom-made chamber was fixed above
335 the NAc in all monkeys; the chamber held a grid that allowed needles to penetrate straight into the
336 NAc without deflecting and potentially entering into other brain areas. At the same time, a
337 platinum ECoG array was chronically implanted in three monkeys (Monkeys M, T, and R). A
338 median linear skin incision was performed on the head, and the skull was exposed over the bilateral
339 frontal cortices. After the round craniotomy, in which the center was located above the NAc, a
340 vinyl chloride or polysulphone chamber was attached to cover the craniotomy. Other craniotomies
341 were located around the central sulcus, and the cortex around the central sulcus was exposed
342 bilaterally in two monkeys (Monkeys M and R) and unilaterally (right) in Monkey T. In Monkeys
343 M and R, the ECoG array, comprised of 15 channel (5 x 3 grid) electrodes, was placed on the digit,
344 hand, and arm areas of the primary motor (M1), primary somatosensory (S1), dorsal aspect of the
345 premotor (PMd), and ventral aspect of the premotor cortex (PMv) on both hemispheres. The ECoG
346 array, which was comprised of 16 channel (4 x 4 grids) electrodes, was placed unilaterally (right)
347 on the same area in Monkey T. The electrodes had a diameter of 1 mm and inter-electrode distance
348 of 4 mm centre-to-centre. Small titanium-steel screws were attached to the skull as anchors. The
349 skull and screws were completely covered with acrylic resin. Two titanium-steel tubes were
350 mounted in parallel over the frontal and occipital lobes for fixation of the head. The chamber was
351 also fixed to the screws by the acrylic resin.

352 2) Spinal cord injury (SCI)

353 Lateral corticospinal tract (l-CST) lesions were established as described previously (*13-*
354 *16*). The l-CST was transected in all monkeys after pre-lesion data were obtained. Under the above-
355 mentioned anaesthesia, the border between the C4 and C5 segments (C4/C5) was exposed by
356 laminectomy of the C3 and C4 vertebrae, and a transverse opening was made in the dural
357 membrane. A small opening was made in the pia mater at the lateral convexity of the spinal cord.
358 A horizontal strip was made in a mediolateral direction relative to the lateral funiculus by inserting
359 a minute L-shaped hook that could not be inserted >5 mm deep, which corresponds to the distance
360 from the lateral convexity of the spinal cord to the midline. The dorsal part of the lateral funiculus
361 was transected from the dorsal root entry zone ventrally to the level of the horizontal strip lesion.
362 The lesion was extended ventrally at the most lateral part of the lateral funiculus (Fig. 1B and fig.
363 S3). The skin and back muscles were sutured with nylon or silk.

364

365 **Inactivation of the NAc**

366 To determine the contribution of the NAc to finger dexterity and brain activity during the
367 reach and grasp task, the NAc in the hemisphere contralesional to the SCI was inactivated
368 pharmacologically at various time points before and after SCI (day-7, 8, 28, 40, 82, and 99 in
369 Monkey D; day-27, -7, 16, 29, 94, 113, and 260 in Monkey M; day-22, 26, 34, 55, and 97 in
370 Monkey T; day-27, 11, 22, 51, 85, 126 and 156 days after SCI in Monkey R). Muscimol, a gamma
371 aminobutyric acid $(GABA)_A$ receptor agonist, was pressure injected at a rate of 0.2 μL/min (8 sites,
372 1 μL/site, 5 μg/μL, dissolved in 0.1 M phosphate buffer, pH 7.4) to accomplish focal inactivation
373 of the contralesional NAc. We then observed changes in brain activity and finger dexterity. A 10-
374 μL Hamilton syringe (Hamilton Company, Reno, Nevada, USA) was held on the syringe pump,

which was fixed on the stereotaxic manipulator. The grid-guided needle was stereotactically inserted into the NAc. The same volume of muscimol was injected into the same sites before and after SCI. Considering that our previous result indicated a 1.5 μL injection of muscimol inactivated a spherical volume of brain tissue 3-4 mm in diameter (*33*), which is consistent with those of other previous studies (*34-36*), injection sites (fig. S1A, B) and muscimol volumes were chosen so that muscimol infiltrated the whole NAc, assuming that 1 μL of muscimol would diffuse within a 2-mm radius. Injection sites were identified by the MRI images. An X-ray photo confirmed that the tip of the needle was placed within the NAc, as considered by the location of pituitary fossa and frontal base, during injection experiment (fig. S1C).

Data collection

1) Simultaneous recording LFP from the NAc and ECoG signals from the SMC

Every time the monkeys perform their task, cortical oscillatory activity on the surface of the SMC was recorded by the ECoG array in three monkeys (M, T and R). In addition, local field potentials (LFPs) in the NAc were recorded simultaneously using four platinum extracellular microelectrodes arranged with 1 mm intervals, which coiled around a tungsten needle of 0.4mm radius. These simultaneous recordings were acquired while the NAc was functioning normally (i.e., not inactivated) and at various time points before and after SCI in two monkeys (day-63, -28, 16, 28, 44, 63, 73, 84, 116 and 119 in monkey R; day-15, 28, 29, 50, 51, 57, 58, 62 and 64 in monkey T). Every time we recorded LFPs from the NAc, we inserted a needle electrode through the grid mentioned above and removed it at the end of the session of the day. Signals were recorded with a Cerebus™ data acquisition system at a sampling rate of 2,000 Hz. ECoG and LFP signals were extracted using multi-channel amplifiers with a band-pass analogue filter (0.3 Hz high-pass and 7,500 Hz low-pass) and with band-pass digital filters in the Neural Signal Processor (0 Hz high-pass and 250 Hz low-pass). Infrared sensors placed on the hand holder and the window allowed us to determine when the monkeys hand was in the rest position and when the food piece was being retrieved.

At the beginning of the present electrophysiological recording study, the electrode on the finger area of the primary motor cortex (M1) was identified by electrical stimulation (fig. S2). ECoG electrodes delivered microstimulation current through a custom made stimulator to evoke finger movements. The electrode on the digit area of M1 was then used for the M1 electrode analysis throughout the experimental period.

2) ECoG recording before and during NAc inactivation

SMC surface activity was recorded by the ECoG array before and during NAc inactivation while the monkeys performed the reach and grasp task in three monkeys (M, T and R). These data were also recorded by the same setup as above.

Analyses

1) Behavioral data analyses

The mean reaching and grasping times were calculated from each session consisted of 30 trials. Then, increasing rate of reaching and grasping time caused by NAc inactivation was calculated for each day of inactivation experiment. The behavioural analyses were made for three stages in each monkey. The first stage was defined as the time period before SCI. The second 'early stage recovery', was defined as the period from SCI to the time point in which the success rate reached 100% for two successive days. The third 'late recovery stage', was defined as the period in which the 100% success rate remained stable. Therefore, such increasing rates of reaching and grasping times by NAc inactivation were classified into three groups (Pre-SCI, Early, Late). Then, the mean increasing rate during each recovery phase was calculated. In addition, we calculated the mean increasing rate caused by the injection of saline, regardless of the recovery phase. A one-way analysis of variance was used to determine the statistical reliability of the time differences. Tukey's Least Significant Difference test was chosen as the post-hoc test (Fig. 3D; $n_{pre\text{-}SCI} = 4$, $n_{early} = 8$, $n_{late} = 7$, $n_{saline} = 6$: $F(3,21) = 5.25$, $P = 0.0074$, ($P = 0.0131$, pre vs early; $P = 0.044$, early vs late; $P = 0.0013$, early vs saline) and E; $n_{pre\text{-}SCI} = 4$, $n_{early} = 7$, $n_{late} = 7$, $n_{saline} = 6$: $F(3,20) = 1.7$, $P = 0.1995$). Each sample size indicates the number of days for inactivation experiments across Monkeys M, T and R). In Monkey M, we couldn't obtain the mean reaching time after NAc inactivation because reaching speed was too slow for us to detect the end of reaching in each trial only on day 29.

2) Electrophysiological data analyses

To estimate ECoG signal changes related to the reach and grasp task, we performed time-frequency decomposition using a MATLAB code written by the authors. We conducted a notch filtering procedure to filter out multiples of the western Japan power supply AC components (60, 120, 180, 240, 300, 360 Hz). The wavelet transform was chosen, and the Molet wavelet was used as the mother wavelet, as the wavelet transform provides high time and frequency resolution. To analyze the brain activity during the dexterous finger movement, time course was aligned at the grasp onset and then produced an event-related time-frequencygram. Brain activity during grasping should be analyzed because finger dexterity plays more critical role during grasping. Then we computed the arithmetic mean of the time-frequencygram of 30 trials. To highlight the change in power for each frequency, power values were standardized in each frequency bin using the mean and standard deviation (SD) of each baseline period. The baseline period was defined as 1 s from the beginning of the time-frequencygram (Upper and middle row in fig. 4B, S4A and B).

For each day of simultaneous recording experiments, mean power increase or decrease for 0.5 second after the grasp onset as compared with baseline period was calculated for each specific band ranges 0–400 Hz based on the time-frequencygrams. Each mean power changes were divided into three groups such as Pre-SCI, Early and Late (Fig. 1E and F; each sample size indicates simultaneous recording days obtained from monkeys T and R). Then, arithmetic mean and S,E,M were calculated for each group. In addition, at each frequency band, a one-way analysis of variance was used to determine the statistical reliability of the time differences (Fig. 1E and F).

To assess the statistical significance of the differences between the pre-inactivation and post-inactivation time-frequencygram, we performed t-tests on values from these two maps. We generated 30 time-frequencygrams with 400 × 3,000 pixels from each session. Therefore, a certain pixel in each map had 30 values from one session. We conducted t-tests to compare the pre-inactivation and post-inactivation clusters of 30 values in all pixels and produced a 'p-value time-frequencygram'. In addition to the p-values, we considered increases and decreases in the power of each pixel on the map (Lower row in fig. 4B, fig. S4A and B).

To evaluate the directionality of interactions between the ECoG signals on the cortical surface and LFPs in the NAc, we employed Granger causality analysis (GCA) using the causal connectivity toolbox (*37*). Granger causality (GC) value indicates strength of connectivity. Clarifying the GC time-change depends on the events; therefore, GCA was performed on the time series of the ECoG and LFP signals within a time window of 1 s before to 0.5 s after the grasping onset. We then generated a GC time-frequencygram. GC spectra were found using scanning steps of 1 s per window (Fig. 2A). GC spectra means were calculated across all recordings collected from two monkeys (R and T). Each spectrum was calculated from the signals acquired during the 1-s window after grasp onset (Fig. 2B).

To clarify whether the changes in ECoG power were widely distributed or localized in the SMC, we investigated the power change in all channels following NAc inactivation. Considering finger dexterity plays more critical role during grasping, we conducted a Fourier transform using an analysis time window of 512 ms (sampling rate was 2,000 Hz) after the grasping onset, and computed the mean power of each rhythmic band of pre-inactivation signals and post-inactivation signals in each electrode (Left and middle column in fig. 4C, S5A and B). Differences were assessed by dividing the post-inactivation power by the pre-inactivation power (Right column in fig. 4C, S5A and B), and a topographic map was generated after smoothing using a 100-point inter-electrode distance.

To examine the differences in the power change pattern between the recovery phases, we calculated the mean power change rate during each recovery phase. These were calculated by dividing the post-inactivation power by the pre-inactivation power for each frequency. To create the power spectrum, we conducted Fourier transform using an analysis time window of 512 ms (sampling rate was 2,000 Hz) after the grasping onset. In addition, at each frequency band, a one-way analysis of variance was used to determine the statistical reliability of the time differences. On the frequency band in which early group was significantly higher than other group, red circles were presented above the panel (Fig. 4D).

3) Histological analysis

We marked the injection sites by electrocoagulation, which was made with a rectangular constant current at 30 μA for 20 s. During the electrocoagulation the monkeys were deeply anaesthetized with sodium pentobarbital (20 mg/kg, i.v.). At the end of all experiments, the monkeys were deeply anaesthetized with an overdose of sodium pentobarbital (50–75 mg/kg, i.v.) and perfused transcardially with 0.1 M phosphate buffered saline (PBS, pH 7.3), followed by 4% paraformaldehyde in 0.1 M PBS (pH 7.3). The spinal cord and brain were immediately removed from the skull and immersed in 30% sucrose solution of 0.1 M PBS (pH 7.3). Serial sections (50μm) of the spinal cord (axial) and brain (coronal) were cut on a freezing microtome. All sections were processed for Nissl-staining with 1% cresyl violet.

We captured the photomicrographs of the spinal cord lesion, and then reconstructed using Adobe Illustrator. The extent of the SCI lesion in the C4/C5 spinal cord was calculated from spinal sections using the following equation: $R=1-\alpha/\beta$, were R is a measure of the lesion extent, where α is the area of white matter without a dorsal funicle on the intact side, and β is the area of white matter without lesion and a dorsal funicle on the affected side (Fig.1B and fig. S3) (*38*).

Muscimol inactivation sites were deduced based on the location of coagulation in coronal sections of the brains (Fig. S1B) of Monkeys M, T, and R. In Monkey D, we estimated the location of inactivation sites based on the insertion tract and magnetic resonance images (Fig. S1A).

Figs. S1 to S6

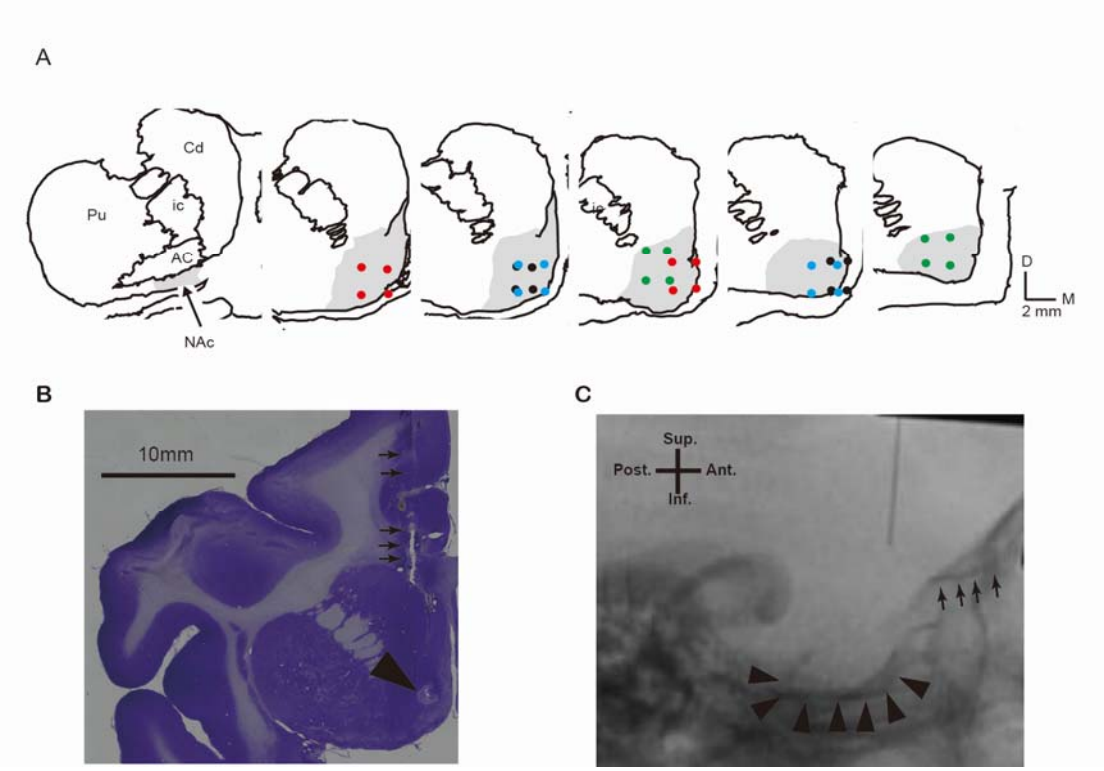

Fig. S1. Illustrations of brain sections including inactivation and recording sites in the nucleus accmubens (NAc). (**A**) Locations of injection and recording sites in four monkeys [Monkey M (Red), T (black), D (green), and R (blue)] are superimposed on six representative coronal sections presented at 1-mm intervals from the anterior edge to the posterior end of the NAc (grey shading). Cd, caudate nucleus; Pu, putamen; ic, internal capsule; AC, anterior commissure; D, dorsal; M, medial. (**B**) A Nissl-stained histological section containing the coagulation scar in the NAc. The black triangle indicates the coagulation scar. The arrowheads indicates the scar of insertion track. (**C**) A lateral view of the X-ray photo showing the injection needle was inserted into the NAc. The black triangles and black arrowheads indicate the pituitary fossa and frontal base, respectively.

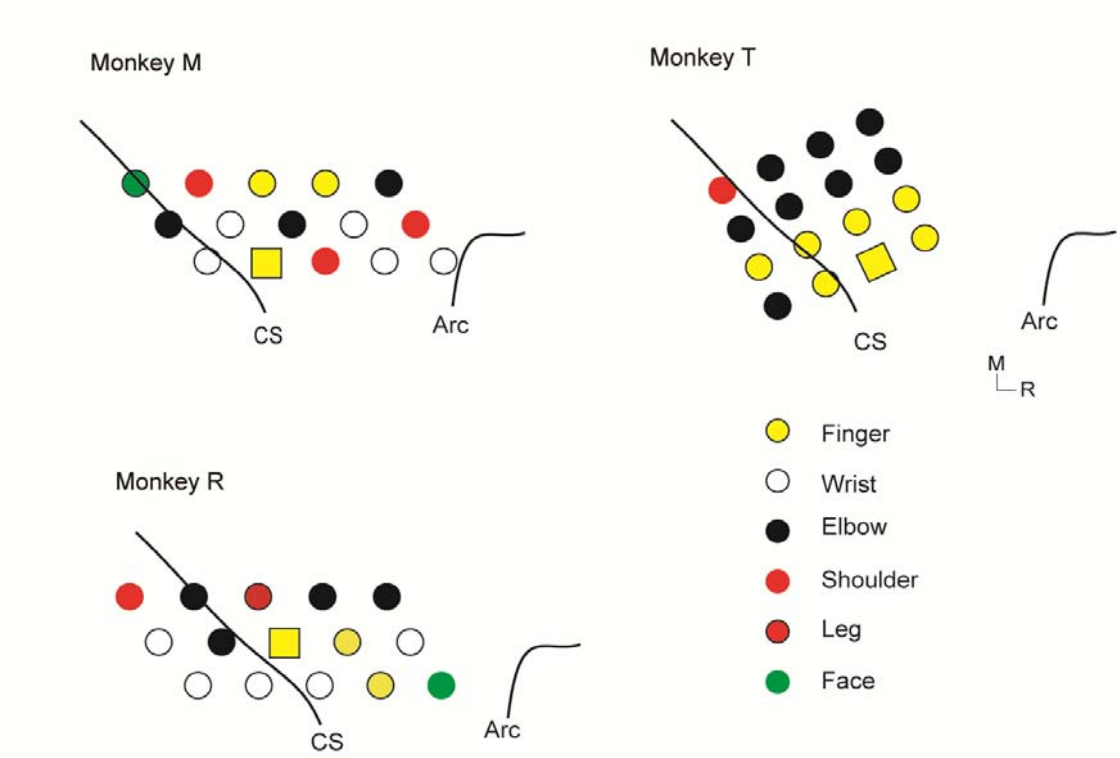

Fig. S2. Location of the electrocorticographic (ECoG) electrode on the contralesional hemisphere. Circles and squares indicate the ECoG electrodes that were placed on the sensorimotor cortex (SMC). Different color and shape combinations indicate the movement evoked by threshold electrical stimulation. The yellow square shown for each monkey denotes the electrode used as the M1 electrode for analysis purposes (See Fig. 1D, 2A, 4A and fig. S4). CS, central sulcus; Arc, arcuate sulcus; R, rostral; M, medial.

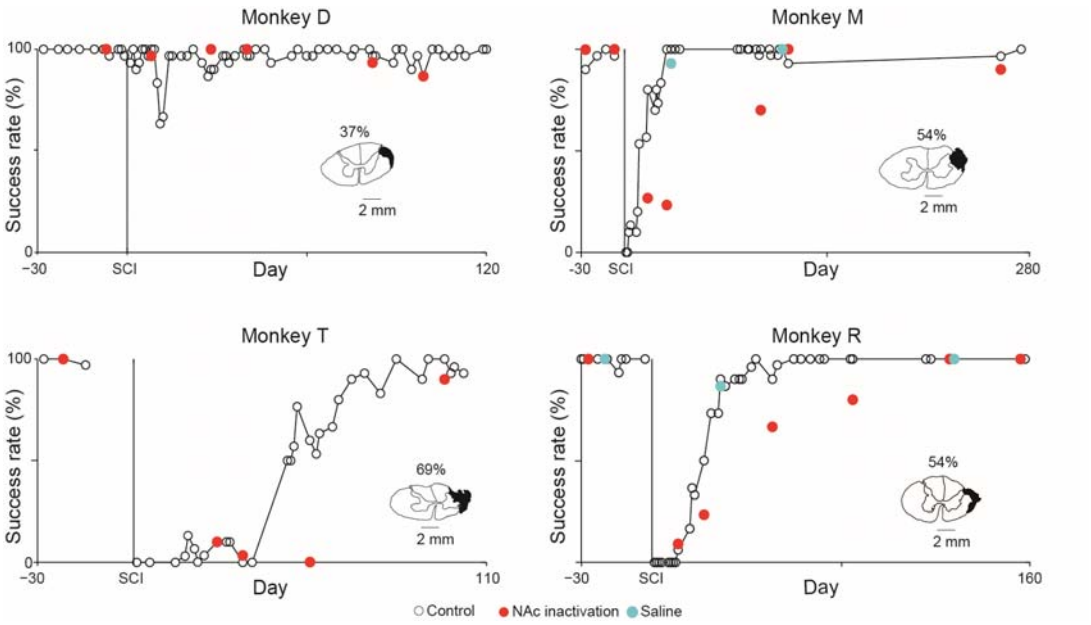

Fig. S3. Recovery time course and NAc inactivation effects on finger dexterity in all monkeys. The vertical and horizontal axes indicate the precision grip success rate and the day relative to the time of the spinal cord injury (SCI), respectively. Outlined circles represent the precision grip success rate in the absence of NAc inactivation. The precision grip success rate during NAc inactivation (red circles) and after saline injection (light blue circles). The black shading in the inset indicates the area of the spinal cord lesion. The percentage value beside the spinal cord illustration shows the proportion of the hemilateral white matter that has been lesioned outside the dorsal funicule.

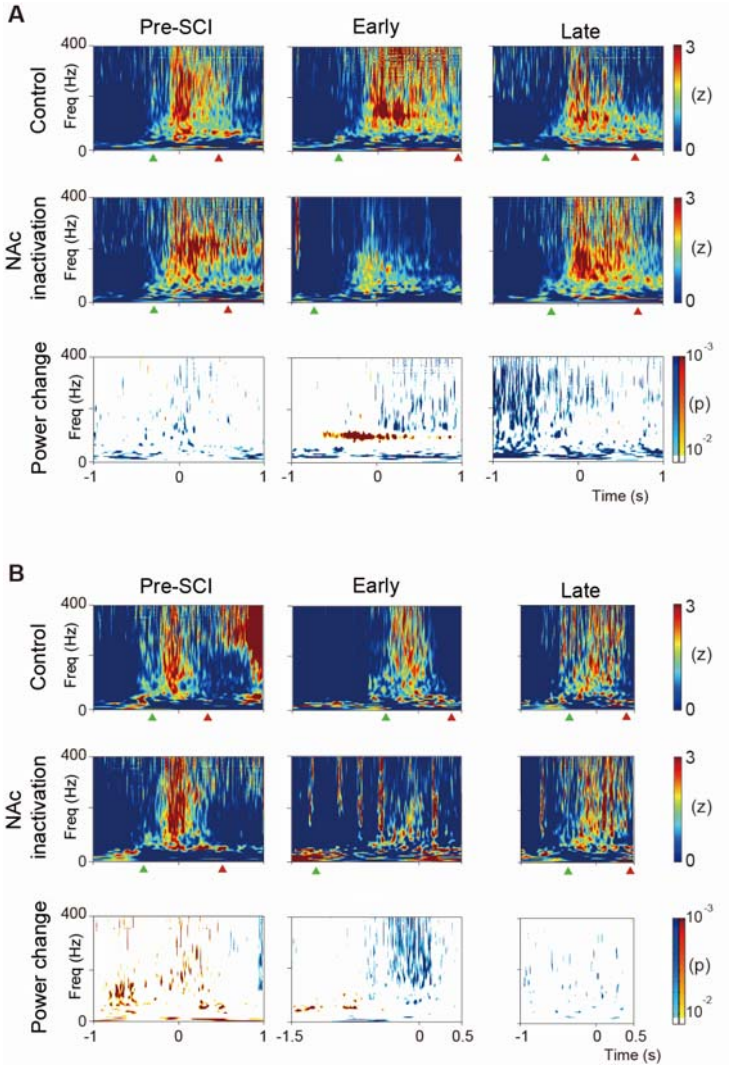

Fig. S4. ECoG signal change induced by inactivation of NAc in two monkeys (T and R). (**A**) Effect of NAc inactivation on M1 activity. Time-frequency analysis of activity in the contralesional finger area of M1 while Monkey T performed the reach and grasp task prior to NAc inactivation (upper row) and during NAc inactivation (middle row) at each recovery stage. Time zero on the horizontal axis represents the onset of grasping. Lower row indicates power change in M1 activity caused by NAc inactivation. Blue and red areas indicate statistically reliable deactivated and activated components, respectively. (**B**) Data obtained from Monkey R.

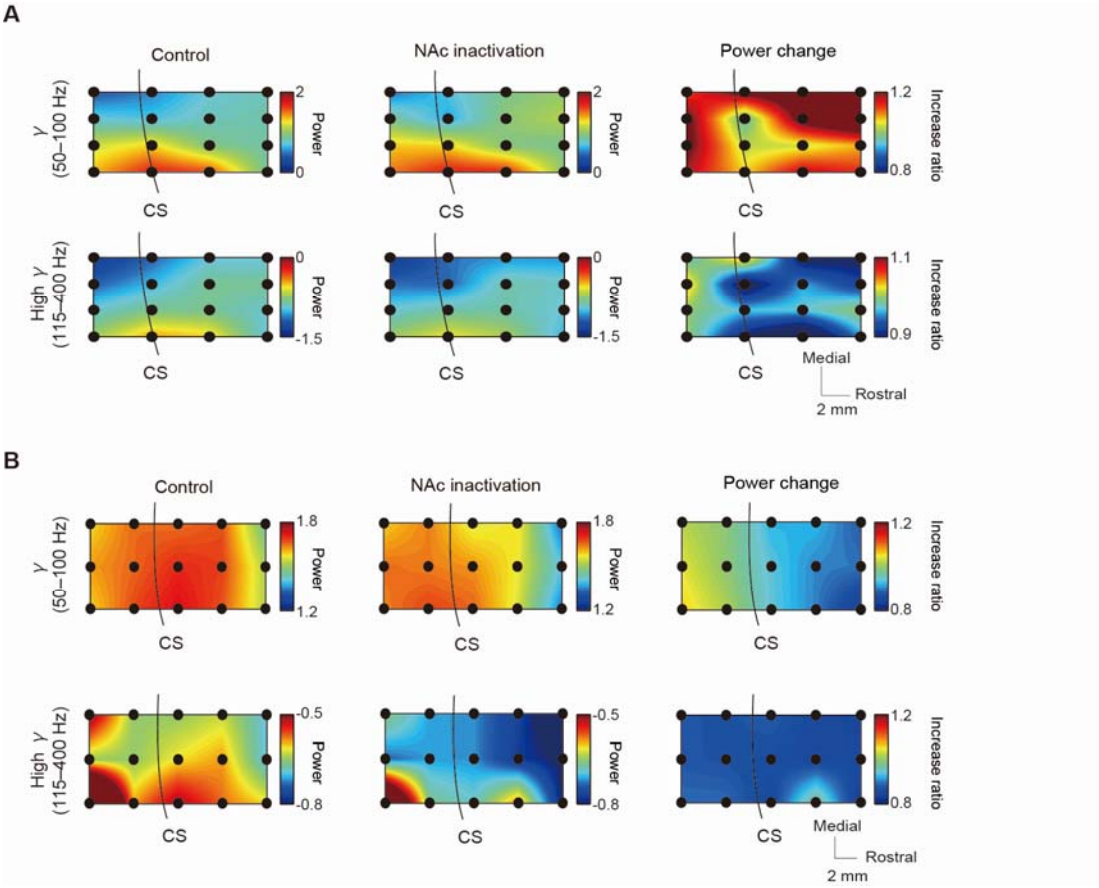

Fig. S5. Global change of gamma and high-gamma power on the SMC. (**A**) Topographical mapping of gamma (50–100 Hz) and high-gamma (115–400 Hz) power intensity before and during NAc inactivation in Monkey T during the early stage of recovery. Each dot on the maps indicates an electrocorticographic (ECoG) electrode (left and middle columns). Right column indicates the mapping of changes in gamma and high-gamma power. (**B**) Data obtained from Monkey R. CS: central sulcus.

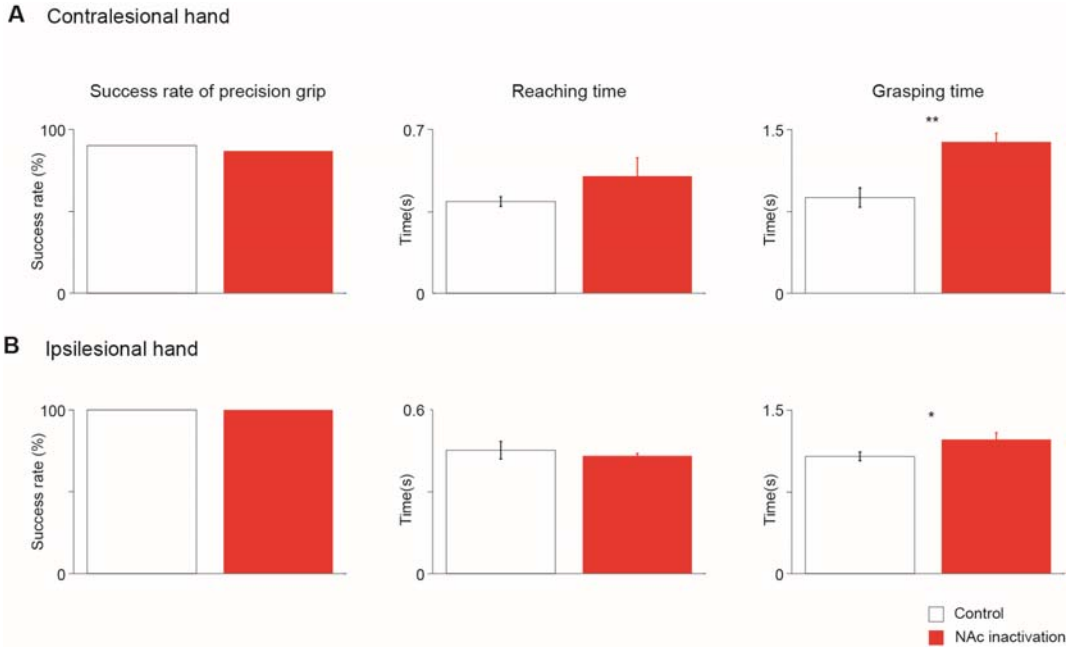

548

549 **Fig. S6.** Effects of unilateral NAc inactivation on finger dexterity. (**A**) Changes in grasp success
550 rate caused by unilateral inactivation of the contralesional NAc in Monkey M, 16 days after SCI
551 (left panel). The center and right panels show changes in the mean reaching and grasping times,
552 respectively. Error bars indicate standard error of the mean (S.E.M.) **P =0.000137, Student's t-
553 test. (**B**) Data obtained from the ipsilesional hand after unilateral inactivation of the ipsilesional
554 NAc in Monkey M, 38 days after SCI. *P = 0.044.

Captions for Movies S1 to S5

Movie S1 Recovery time course of finger dexterity. This video shows that a monkey grabbed pieces of sweet potato before and after the SCI. Before the SCI, the monkey grabbed food piece with precision grip using index finger and thumb. Just after the SCI, it could not retrieve the food. At early stage, it grabbed the food, though it seemed still clumsy. At late stage, precision grip recovered completely.

Movie S2 Effect of NAc inactivation on recovery of finger dexterity. Monkey could grab a piece of food after 16 days after the SCI (Early stage). However, inactivation of NAc caused severe weakness on the affected hand.

Movie S3 Effect of NAc inactivation on intact monkey. Inactivation of NAc didn't have influence on the intact monkey (Pre-SCI).

Movie S4 Effect of NAc inactivation on recovered finger dexterity. Inactivation of NAc didn't have influence on the affected hand 113 days after the SCI (late stage).

Movie S5 Effect of NAc inactivation on contralesional (intact) hand after the SCI. Monkey could grab pieces of food using contralesional (intact) hand even during inactivation of the contralesional NAc 16 days after the SCI.